

## Sticking transition in a minimal model for the collisions of active particles in quantum fluids

Vishwanath Shukla,<sup>1,2,\*</sup> Marc Brachet,<sup>3,†</sup> and Rahul Pandit<sup>2,‡</sup>

<sup>1</sup>Laboratoire de Physique Statistique de l'Ecole Normale Supérieure, 24 Rue Lhomond, 75231 Paris, France

<sup>2</sup>Centre for Condensed Matter Theory, Department of Physics, Indian Institute of Science, Bangalore 560012, India

<sup>3</sup>Laboratoire de Physique Statistique de l'Ecole Normale Supérieure, associé au CNRS et aux Universités Paris VI et VII, 24 Rue Lhomond, 75231 Paris, France

(Received 18 March 2016; revised manuscript received 11 August 2016; published 19 October 2016)

Particles of low velocity, traveling without dissipation in a superfluid, can interact and emit sound when they collide. We propose a minimal model in which the equations of motion of the particles, including a short-range repulsive force, are self-consistently coupled with the Gross-Pitaevskii equation. We show that this model generates naturally an effective superfluid-mediated attractive interaction between the particles; and we study numerically the collisional dynamics of particles as a function of their incident kinetic energy and the length scale of the repulsive force. We find a transition from almost elastic to completely inelastic (sticking) collisions as the parameters are tuned. We find that aggregation and clustering result from this sticking transition in multiparticle systems.

DOI: 10.1103/PhysRevA.94.041602

Studies of an assembly of particles in a superfluid have a rich history [1]. This challenging problem is of relevance to recent experiments on particles in superfluid helium [2–6] and impurities in cold-atom Bose-Einstein condensates (BECs) [7]. Its understanding requires models and techniques from the physics of quantum fluids with state-of-the-art methods from theoretical and numerical studies of turbulence. In contrast to particles moving through a viscous fluid, particles move through a zero-temperature superfluid without dissipation, so long as they travel at speeds lower than the critical speed above which the particles shed quantum vortices [8–10]. The motion of a single particle, which is affected by the superflow and acts on it too, has been studied in Ref. [11] in a Gross-Pitaevskii (GP) superfluid. We refer to this as an *active particle*.

We go well beyond earlier studies [11–13] of this problem by developing a minimal model. We introduce *active and interacting* particles in the Gross-Pitaevskii Lagrangian that describes a weakly interacting superfluid at zero temperature. By using this model we show that even if particles move through the superfluid at subcritical speeds, they can dissipate energy when they collide, because a two-particle collision excites sound waves; clearly the coefficient of restitution  $e < 1$  for such a collision. We show that our model leads naturally to a superfluid-mediated attraction between the particles. We calculate this attraction both approximately, via a Thomas-Fermi approximation, and numerically, from a direct numerical simulation (DNS) of the Gross-Pitaevskii equation (GPE). We show that the interplay between the short-range (SR) particle repulsion, which we have included in our Lagrangian, and the superfluid-mediated (SM) attraction leads to a *sticking* transition at which the coefficient of restitution  $e$  for two-particle collisions vanishes. We develop a simple, mean-field theory for this transition and we compare it with our DNS results. Furthermore, we elucidate the rich dynamical behaviors of (a) two-particle collisions in the superfluid, when

the impact parameter  $b$  is nonzero, and (b) assemblies of particles, which aggregate because of the SM attraction. We present illustrative calculations in two dimensions (2D).

To study the dynamics of particles in a Bose superfluid, we propose the Lagrangian

$$\begin{aligned} \mathcal{L} = \int_{\mathcal{A}} \left[ \frac{i\hbar}{2} \left( \psi^* \frac{\partial \psi}{\partial t} - \psi \frac{\partial \psi^*}{\partial t} \right) - \frac{\hbar^2}{2m} \nabla \psi \cdot \nabla \psi^* + \mu |\psi|^2 \right. \\ \left. - \frac{g}{2} |\psi|^4 - \sum_{i=1}^{\mathcal{N}_0} V_{\mathcal{P}}(\mathbf{r} - \mathbf{q}_i) |\psi|^2 \right] d\mathbf{r} + \frac{m_o}{2} \sum_{i=1}^{\mathcal{N}_0} \dot{q}_i^2 \\ - \sum_{i,j,i \neq j}^{\mathcal{N}_0, \mathcal{N}_0} \frac{\Delta E r_{\text{SR}}^{12}}{|\mathbf{q}_i - \mathbf{q}_j|^{12}}, \end{aligned} \quad (1)$$

where  $\psi$  is the complex, condensate wave function,  $\psi^*$  its complex conjugate,  $\mathcal{A}$  the simulation domain,  $g$  the effective interaction strength,  $m$  the mass of the bosons,  $\mu$  the chemical potential,  $V_{\mathcal{P}}$  the potential that we use to represent the particles, and  $\mathcal{N}_0$  the total number of particles with mass  $m_o$ . The last term in Eq. (1) is the SR repulsive, two-particle potential; we treat  $\Delta E$  and  $r_{\text{SR}}$  as parameters.

The Lagrangian (1) yields the GPE

$$i\hbar \frac{\partial \psi}{\partial t} = -\frac{\hbar^2}{2m} \nabla^2 \psi - \mu \psi + g |\psi|^2 \psi + \sum_{i=1}^{\mathcal{N}_0} V_{\mathcal{P}}(\mathbf{r} - \mathbf{q}_i) \psi; \quad (2)$$

and the equation of motion for the particle  $i$

$$m_o \ddot{\mathbf{q}}_i = \mathbf{f}_{o,i} + \mathbf{f}_{\text{SR},i}, \quad (3)$$

where

$$\mathbf{f}_{o,i} = \int_{\mathcal{A}} |\psi|^2 \nabla V_{\mathcal{P}} d\mathbf{r}; \quad (4)$$

$\mathbf{f}_{\text{SR},i}$  arises from the SR repulsive potential [the last term in Eq. (1)]. In the absence of any external force, the total energy of this system is conserved. Moreover, the dynamical evolution of the coupled set of Eqs. (2) and (3) conserves the total momentum and the number of bosons, which constitute the superfluid. We can express the GP in terms of hydrodynamical

\*research.vishwanath@gmail.com

†brachet@physique.ens.fr

‡rahul@physics.iisc.ernet.in; also at Jawaharlal Nehru Centre For Advanced Scientific Research, Jakkur, Bangalore, India.

variables by using the Madelung transformation  $\psi(\mathbf{r}, t) = \sqrt{\rho(\mathbf{r}, t)/m} \exp[i\phi(\mathbf{r}, t)]$ , where  $\rho(\mathbf{r}, t)$  and  $\phi(\mathbf{r}, t)$  are the density and phase fields, respectively; the superfluid velocity is  $\mathbf{v}(\mathbf{r}, t) = (\hbar/m)\nabla\phi(\mathbf{r}, t)$ , which shows that the motion is irrotational in the absence of any vortices. We represent a particle by the Gaussian potential  $V_P = V_o \exp(-r^2/2d_p^2)$ ; here  $V_o$  and  $d_p$  are the strength of the potential and its width, respectively. The particle displaces some superfluid with an area of the order of the particle area; we denote the mass of the displaced superfluid by  $m_f$ . We use the ratio  $\mathcal{M} \equiv m_o/m_f$  to define three types of particles: (1) heavy ( $\mathcal{M} > 1$ ), (2) neutral ( $\mathcal{M} = 1$ ), and (3) light ( $\mathcal{M} < 1$ ).

To solve Eqs. (2) and (3) numerically, we use a pseudospectral method with the 2/3-dealiasing rule [14,15] on a 2D, periodic, computational domain of side  $L = 2\pi$ , i.e.,  $\mathcal{A} = L^2$ ; we use a fourth-order Runge-Kutta scheme for time marching. We work with the quantum of circulation  $\kappa \equiv h/m \equiv 4\pi\alpha_0$ , speed of sound  $c = \sqrt{2\alpha_0 g \rho_0}$ , healing length  $\xi = \sqrt{\alpha_0/(g\rho_0)}$ , and mean density  $\rho_0$ . In all our calculations, we set  $\rho_0 = 1$ ,  $c = 1$ , and  $\xi = 1.44 dx$ , where  $dx = L/N_c$ ,  $N_c^2 = 128^2$  is the number of collocation points,  $\mu = g$ ,  $V_o = 10g$ ,  $d_p = 1.5\xi$ , and  $\Delta_E = 0.062$ . (See Supplemental Material [16].)

We first examine a head-on, two-particle collision. We prepare an initial state with two neutral particles, at rest, separated by  $r_0 = 7\xi$  in the superfluid [17]. We evolve this state by using the GPE in the presence of the SR repulsion between the particles, with  $r_{SR} = 1.5\xi$ , after they are released from rest at  $t = 0$ . In Fig. 1(a) we plot the particle positions versus the scaled time  $ct/\xi$ . In the insets of Fig. 1(a), we show pseudocolor plots of  $\rho(\mathbf{r})$  at times labeled (i)–(vi); these plots show sound waves after the collision between the particles, which appear as blue disks with  $\rho = 0$ . We see that the particles accelerate toward each other and stop on collision, when the separation  $r \simeq r_{SR}$ ; and then their motion is reversed, but they do not escape to infinity and undergo multiple collisions, which

are accompanied by acoustic emission, until they lose their initial kinetic energy and they stick to form a bound pair; i.e., we have an inelastic collision (Video M1, Supplemental Material [16]).

To characterize the SM attractive potential between the particles [18], we write the total energy contained in the superfluid field as

$$E_F = \frac{1}{\mathcal{A}} \int_{\mathcal{A}} \left[ \frac{\hbar^2}{2m} |\nabla\psi|^2 + \frac{g}{2} \left( |\psi|^2 - \frac{\mu}{g} \right)^2 + \sum_{i=1}^{N_o} V_P(\mathbf{r} - \mathbf{q}_i) |\psi|^2 \right] d\mathbf{r}. \quad (5)$$

We now perform DNSs in which we vary the initial scaled distance  $r/\xi$  between the particles; we then obtain  $E_F(r/\xi)$ , the energy of the minimum-energy state without the SR repulsion, by using the imaginary-time procedure [17]. In Fig. 1(b), we plot the potential  $U_A = E_F(r) - E_F(r = \infty)$  versus  $r/\xi$ ;  $U_A$  is negative (i.e., attractive), for small  $r/\xi$  and vanishes in the limit  $r/\xi \rightarrow \infty$ .

We can estimate  $U_A(r/\xi)$  for the two-particle case by using the Thomas-Fermi (TF) approximation [19] as follows. We neglect the kinetic-energy term in Eq. (2) and write

$$|\psi(\mathbf{r})|^2 = (\mu - \mathcal{V}_P)\theta(\mu - \mathcal{V}_P)/g, \quad (6)$$

with  $\mathcal{V}_P = V_P(\mathbf{r} - \mathbf{q}_1) + V_P(\mathbf{r} - \mathbf{q}_2)$  and  $\theta$  the Heaviside function that ensures  $|\psi|^2 > 0$ . In this approximation,

$$E_F^{\text{TF}} = \frac{1}{\mathcal{A}} \int_{\mathcal{A}} [\mu^2 - (\mu - \mathcal{V}_P)^2 \theta(\mu - \mathcal{V}_P)] / (2g) d\mathbf{r}; \quad (7)$$

$U_A^{\text{TF}} = E_F^{\text{TF}}(r) - E_F^{\text{TF}}(r = \infty)$ , which we plot in the inset of Fig. 1(b) versus  $r/\xi$ . It is in qualitative agreement with  $U_A$  from our DNS; the quantitative difference arises because the TF approximation neglects the kinetic-energy term in Eq. (2).

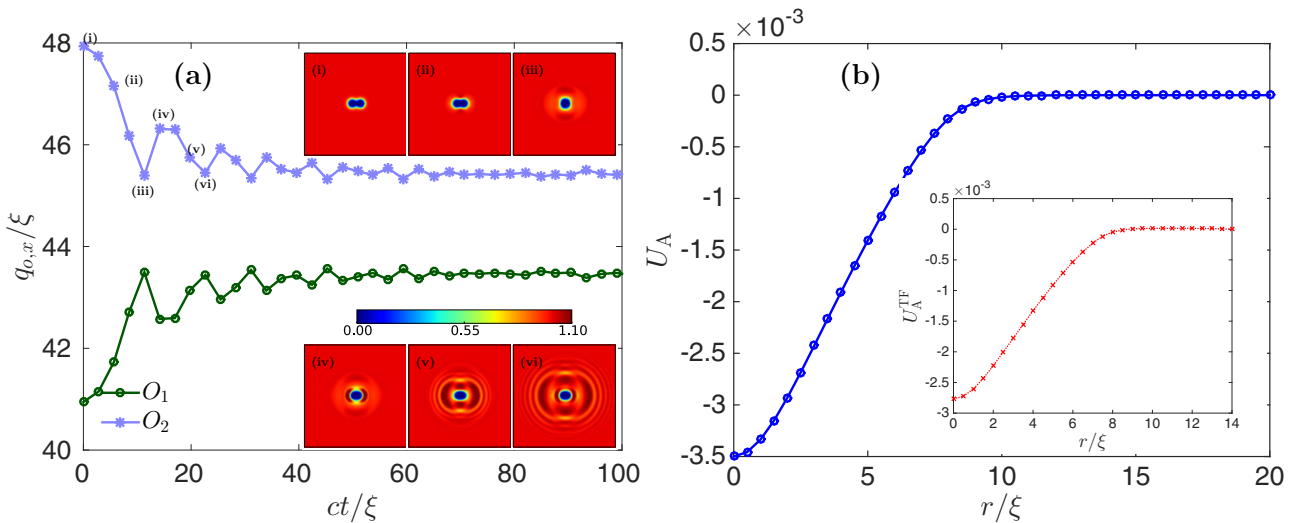


FIG. 1. Superfluid-mediated attractive potential: (a) Plot of the particle ( $\mathcal{M} = 1$ ) positions  $q_{o,x}$  vs the scaled time  $ct/\xi$ . Inset: the sequence of the collision events shown via the pseudocolor plots of the density field  $\rho(\mathbf{r})$  (the particles appear as blue disks in which  $\rho = 0$ ); particles are released from rest, with an initial separation  $r_0 = 7\xi$ , they undergo multiple collisions with the generation of sound waves in the wake of this collision; and they form a bound state with  $r \simeq r_{SR}$ ;  $O_1$  and  $O_2$  are the particle labels. (b) Plot of the superfluid-mediated attractive potential  $U_A$  vs the separation between the particles  $r/\xi$  obtained from our DNSs; the inset shows the same plot, but evaluated by using the Thomas-Fermi approximation Eq. (7). Energies are in units of  $E_\xi = 2\alpha_0 \rho_0^2 g$ .

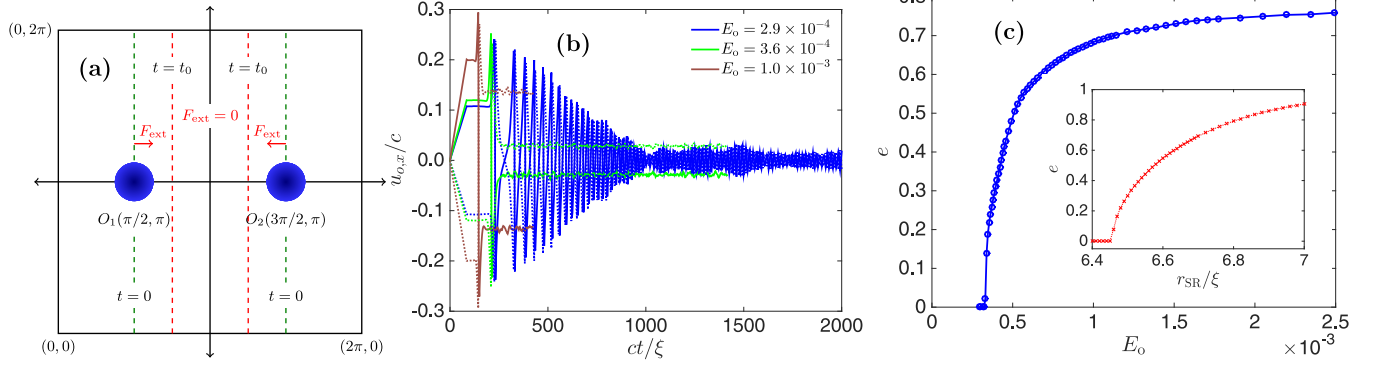


FIG. 2. Head-on collisions: (a) Schematic diagram outlines the initial configuration and the procedure that we use to study the head-on collision between two particles (blue disks). (b) Plots of the particle velocity  $u_{o,x}$  versus  $t$  following a head-on collisions between two heavy particles ( $\mathcal{M} = 7.5$ ) for three different values of the incident kinetic energy  $E_o$  of each particle, at  $r_{SR} = 1.5\xi$ . (c) Plot of the coefficient of restitution  $e$  (Eq. (8)) versus  $E_o$ , for the head-on collision between two heavy particles ( $\mathcal{M} = 7.5$ ). The inset shows  $e$  versus  $r_{SR}/\xi$ , but for two neutral particles ( $\mathcal{M} = 1$ ).

We now study two simplified cases: (1) head-on collisions, with impact parameter  $b = 0$  and (2) collisions with finite but small  $b$ . The schematic diagram in Fig. 2(a) outlines our procedure. We use an initial state with two stationary particles:  $O_1$  at  $(\pi/2, \pi)$  and  $O_2$  at  $(3\pi/2, \pi)$ . We apply the external forces  $F_{\text{ext}} = F_0 \hat{x}$  and  $F_{\text{ext}} = -F_0 \hat{x}$ , respectively, to accelerate the particles; and then we turn off  $F_{\text{ext}}$  at  $t = t_0$  [red vertical line in Fig. 2(a)]. In Fig. 2(b) we plot particle velocities  $u_{o,x}(t)$ , from our DNS with two heavy particles ( $\mathcal{M} = 7.5$  and  $r_{SR} = 1.5\xi$ ), for three different values of the incident kinetic energy  $E_o$  of each particle. For  $E_o = 2.9 \times 10^{-4}$  [blue (black) curves in Fig. 2(b)], the behavior of  $u_{o,x}(t)$  is similar to that of neutral-particle collisions with SR repulsion [Fig. 1(a)]; the collision is completely inelastic and the particles form a bound pair; and the separation between their centers fluctuates around  $r \simeq r_{SR}$ . Figure 2(b) shows that for  $E_o = 3.6 \times 10^{-4}$  [green (light gray) curves], the two particles rebound, with small nonzero mean velocities; at the time of the collision, most of the energy is transferred to the repulsive term because of the change in  $E_F(t) - E_F(t_0)$  and  $E_o$  (see the Supplemental Material [16]). After the collision, most of the energy is transferred back to the fluid and the particles have a small kinetic energy. For higher values, e.g.,  $E_o = 1.0 \times 10^{-3}$  [magenta (dark gray) curves], the head-on collision between the heavy particles is nearly elastic; and the particles rebound with velocities that are significant fractions of their values at incidence (Videos M2, M3, and M4 in the Supplemental Material [16]).

We characterize this inelastic-elastic transition by calculating the coefficient of restitution for head-on collisions:

$$e = \frac{u_{2,F} - u_{1,F}}{u_{1,I} - u_{2,I}}, \quad (8)$$

where  $u_{1,I}$  and  $u_{2,I}$  are, respectively, the mean velocities of the particles  $O_1$  and  $O_2$  before the collision and  $u_{1,F}$  and  $u_{2,F}$  are the mean velocities of these particles after the collision. For the collisions described above, we find (1)  $e \simeq 0$  for  $E_o = 2.9 \times 10^{-4}$ ; (2)  $e \simeq 0.24$  for  $E_o = 3.6 \times 10^{-4}$ ; and (3)  $e \simeq 0.68$  for  $E_o = 1.0 \times 10^{-3}$ . In Fig. 2(c) we plot  $e$  versus  $E_o$ . At low values of  $E_o$ , the collision is inelastic with  $e = 0$ ; and as we increase  $E_o$ ,  $e$  becomes finite at a critical value

$E_o \simeq 3.3 \times 10^{-4}$ , and then there is a steep increase followed by a slow, asymptotic growth toward a value close to 1. We observe a similar inelastic-elastic transition, when instead of  $E_o$ , we vary  $r_{SR}/\xi$ ; here we consider neutral particles ( $\mathcal{M} = 1$ ) to illustrate that the sticking transition does not necessarily require heavy particles. The plot of  $e$  versus  $r_{SR}/\xi$  in the inset of Fig. 2(c) shows that at low values of  $r_{SR}/\xi$ , the collision is inelastic with  $e = 0$ ; and as we increase  $r_{SR}/\xi$ ,  $e$  becomes finite at a critical value  $r_{SR}/\xi \simeq 6.46$ , and finally attains a value close to 1.

Our data are consistent with a *continuous sticking transition* at which  $e$  goes to zero continuously as a power  $\beta$  of the control parameter (either  $E_o$  or  $r_{SR}/\xi$ ). We now give a mean-field calculation of this power-law exponent  $\beta$ . The symmetry of these head-on collisions allows us to write  $u_I \simeq -u_{1,I} \simeq u_{2,I}$  and  $u_F \simeq u_{1,F} \simeq -u_{2,F}$ . The energy balance between the states, before and after the collision, is  $E_{\text{rad}}(u_I) + m_o u_F^2 = m_o u_I^2$ , where  $E_{\text{rad}}$  is the energy radiated into sound waves. Therefore,

$$e(u_I) = \sqrt{1 - E_{\text{rad}}(u_I)/m_o u_I^2}, \quad (9)$$

which yields the critical velocity  $u_I^c$  at which  $e(u_I^c)$  first becomes nonzero. In a simple, mean-field approximation, the Taylor expansion of  $E_{\text{rad}}(u_I)$ , around  $u_I = u_I^c$ , yields the mean-field (MF) exponent  $\beta^{\text{MF}} = 1/2$ . Our DNSs yield values of  $\beta$  that are comparable to, but different from,  $\beta^{\text{MF}} = 1/2$ . The calculation of  $\beta$  for this sticking transition, beyond our mean-field theory, and its universality, if any, is a challenging problem.

In Fig. 3(a) we show the trajectories of two heavy particles ( $\mathcal{M} = 7.5$  and  $r_{SR} = 1.5\xi$ ) that collide with each other, with an impact parameter  $b > 0$ . If the incident kinetic energy of the particles is sufficiently high, e.g.,  $E_o \simeq 1.7 \times 10^{-3}$ , they do not stick; the particles get deflected from their incident trajectory at an angle  $\Theta$ , which depends on  $b$  [see Fig. 3(a) for  $b = 2\xi$  and  $b = 4\xi$ ]. However, for  $b = 2\xi$  with  $E_o \simeq 1.8 \times 10^{-5}$ , the incident kinetic energy is small enough to allow the formation of a bound pair [red (center black) curves in Fig. 3(a)]; the inset shows an enlarged version of the particle trajectories, after the collision, with red solid (dashed) curves for particle  $O_1$  ( $O_2$ ).

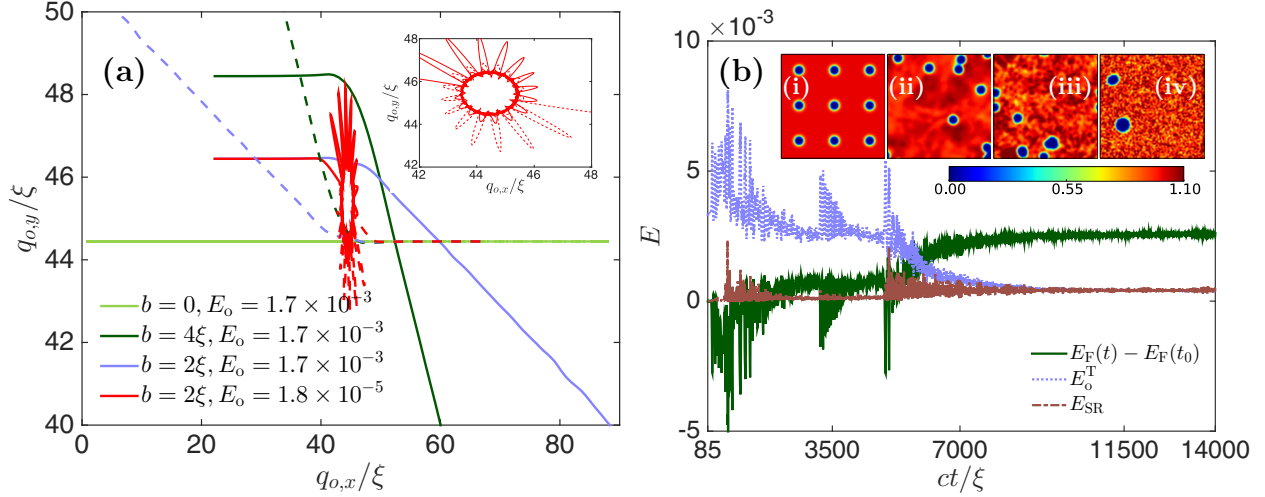


FIG. 3. (a) Collisions at impact parameters  $b \geq 0$ . Light green (light gray), dark green (top black), and blue (gray) curves show the particle trajectories for two heavy particles ( $\mathcal{M} = 7.5$ )  $O_1$  (solid curves) and  $O_2$  (dashed curves) colliding at  $b = 0$ ,  $b = 4\xi$ , and  $b = 2\xi$ , respectively, with incident kinetic energy  $E_o \simeq 1.7 \times 10^{-3}$ . For  $b = 2\xi$  and  $E_o = 1.8 \times 10^{-5}$ , the colliding particles stick to form a bound pair [red (center black) curves]; the inset shows an enlarged view of the particle trajectories for the bound pair, the particle motion is a quasiperiodic function of time. (b) Aggregation. Plots of the time evolution of  $E_F(t) - E_F(t_0)$ , the total kinetic energy  $E_o^T$ , and the total repulsion energy  $E_{SR}$  for nine heavy particles ( $\mathcal{M} = 7.5$ ) initially placed on a lattice; these are set into motion by the application of constant-in-time forces, random in magnitude and direction, for a short duration  $t \leq t_0 \sim 85$  (in units of  $\xi/c$ ). The insets (i)–(iv) illustrate multiparticle collisional dynamics at the representative times  $t_{(i)} = 0 < t_{(ii)} < t_{(iii)} < t_{(iv)}$  by pseudocolor plots of the density field  $\rho(\mathbf{r})$ ; the particles appear as blue disks in which  $\rho = 0$ . Energies are in units of  $E_\xi = 2\alpha_0 \rho_0^2 g$ .

The *sun-flower-petal* pattern of these trajectories indicates that after transients have decayed, the damped oscillatory motion of the particles in the bound pair is akin to that of a dimer, with vibrational and rotational degrees of freedom. The power spectra of the time series  $q_{i,j}(t)$ , for particle  $i \in \{1,2\}$  and coordinate  $j \in \{x,y\}$ , show three prominent frequencies,  $\omega_a = 0.0185c/\xi$ ,  $\omega_b = 0.0148c/\xi$ , and  $\omega_c = 0.0222c/\xi$ , with  $2\omega_a = \omega_b + \omega_c$ , i.e., the oscillatory motion is quasiperiodic (data not shown).

If we start with more than two particles, then a succession of inelastic collisions can lead to the formation of multiparticle aggregates. We illustrate this in Fig. 3(b) for an assembly of nine particles ( $\mathcal{M} = 7.5$  and  $r_{SR} = 1.5\xi$ ); to initialize the system, we place the particles on a lattice [inset (i)] and set them into motion by applying constant-in-time forces, with random magnitudes and directions, for a given duration, such that the collisions occur only after the forces are switched off at  $t = t_0$ . In Fig. 3(b) we plot  $E_F(t) - E_F(t_0)$ , the total kinetic energy  $E_o^T$ , and the total repulsion energy  $E_{SR}$  versus  $ct/\xi$ ; large spikes in these plots occur at collisions; subsequent rearrangements into clusters give rise to strong fluctuations in  $E_{SR}$ ; as the clusters settle into their optimal configurations, the fluctuations in  $E_{SR}$  decrease until they saturate toward the end of our DNS. The pseudocolor plots of  $\rho(\mathbf{r})$  in the insets (ii)–(iv) of Fig. 3(b) show the aggregation of particles (Video M5 in the Supplemental Material [16]).

In conclusion, our minimal model of active and interacting particles in the Gross-Pitaevskii superfluid yields remarkable results, such as the sticking transition and rich aggregation dynamics of particle assemblies. Our qualitative results should hold even in superfluids like helium, in BECs [20], and in three dimensions (we discuss this in the Supplemental Material [16]). Particles in superfluids have been considered by using Biot-Savart methods [13,21–23] and a two-fluid model [24]; the GPE has been studied with a single spherical particle [11]; however, these studies have not considered the collisions and aggregation we elucidate. Impurities in BECs [25] have been described in terms of generalized Bose-Hubbard models, but these works do not study the problems we consider; however, it is an active area of research [26–30]. We hope our work will lead to experimental studies of particle collisions and aggregation in superfluids and BECs.

We thank the Supercomputing Education and Research Centre, IISc, India, for computational resources. V.S. and R.P. thank ENS, Paris, for hospitality, and M.B. thanks IISc, Bangalore, for hospitality. We thank the Council of Scientific and Industrial Research (India), University Grants Commission (India), Department of Science and Technology (India), and the Indo-French Centre for Applied Mathematics for financial support. V.S. acknowledges support from Centre Franco-Indien pour la Promotion de la Recherche Avancée (CEFIPRA/IFCPAR) Project No. 4904.

- [1] R. J. Donnelly, *Quantized Vortices in Helium II*, Vol. 2 (Cambridge University, New York, 1991).  
 [2] G. P. Bewley, D. P. Lathrop, and K. R. Sreenivasan, *Nature* **441**, 588 (2006).

- [3] G. P. Bewley, M. S. Paoletti, K. R. Sreenivasan, and D. P. Lathrop, *Proc. Natl. Acad. Sci. U.S.A.* **105**, 13707 (2008).  
 [4] G. P. Bewley, K. R. Sreenivasan, and D. P. Lathrop, *Exp. Fluids* **44**, 887 (2008).

- [5] D. E. Zmeev, F. Pakpour, P. M. Walmsley, A. I. Golov, W. Guo, D. N. McKinsey, G. G. Ihas, P. V. E. McClintock, S. N. Fisher, and W. F. Vinen, *Phys. Rev. Lett.* **110**, 175303 (2013).
- [6] M. La Mantia and L. Skrbek, *Phys. Rev. B* **90**, 014519 (2014).
- [7] N. Spethmann, F. Kindermann, S. John, C. Weber, D. Meschede, and A. Widera, *Phys. Rev. Lett.* **109**, 235301 (2012).
- [8] T. Frisch, Y. Pomeau, and S. Rica, *Phys. Rev. Lett.* **69**, 1644 (1992).
- [9] C. Nore, C. Huepe, and M. E. Brachet, *Phys. Rev. Lett.* **84**, 2191 (2000).
- [10] T. Winiecki, B. Jackson, J. F. McCann, and C. S. Adams, *J. Phys. B: At. Mol. Opt. Phys.* **33**, 4069 (2000).
- [11] T. Winiecki and C. S. Adams, *Europhys. Lett.* **52**, 257 (2000).
- [12] G. E. Astrakharchik and L. P. Pitaevskii, *Phys. Rev. A* **70**, 013608 (2004).
- [13] E. Varga, C. F. Barenghi, Y. A. Sergeev, and L. Skrbek, *J. Low Temp. Phys.* **183**, 215 (2016).
- [14] G. D. and S. A. Orszag, *Numerical Analysis of Spectral Methods* (SIAM, Philadelphia, 1977).
- [15] V. Shukla, M. Brachet, and R. Pandit, *New J. Phys.* **15**, 113025 (2013).
- [16] See Supplemental Material at <http://link.aps.org/supplemental/10.1103/PhysRevA.94.041602> for the videos and additional figures.
- [17] We prepare such a state by specifying the locations of the particle  $q_i$  in Eq. (2), with  $t$  replaced by  $-it$ , and integrate it to obtain the ground state. This procedure yields states whose initial temporal evolution, in the GPE, produces minimal sound emission. See Refs. [31,32].
- [18] A. Klein and M. Fleischhauer, *Phys. Rev. A* **71**, 033605 (2005).
- [19] C. J. Pethick and H. Smith, *Bose-Einstein Condensation in Dilute Gases* (Cambridge University, New York, 2001).
- [20] N. G. Berloff, M. Brachet, and N. P. Proukakis, *Proc. Natl. Acad. Sci. U.S.A.* **111**, 4675 (2014).
- [21] D. Kivotides, C. F. Barenghi, and Y. A. Sergeev, *Phys. Rev. B* **77**, 014527 (2008).
- [22] D. Kivotides, Y. A. Sergeev, and C. F. Barenghi, *Phys. Fluids* **20**, 055105 (2008).
- [23] Y. Mineda, M. Tsubota, Y. A. Sergeev, C. F. Barenghi, and W. F. Vinen, *Phys. Rev. B* **87**, 174508 (2013).
- [24] D. R. Poole, C. F. Barenghi, Y. A. Sergeev, and W. F. Vinen, *Phys. Rev. B* **71**, 064514 (2005).
- [25] A. Klein, M. Bruderer, S. R. Clark, and D. Jaksch, *New J. Phys.* **9**, 411 (2007).
- [26] F. M. Cucchietti and E. Timmermans, *Phys. Rev. Lett.* **96**, 210401 (2006).
- [27] M. Bruderer, A. Klein, S. R. Clark, and D. Jaksch, *New J. Phys.* **10** (2008).
- [28] D. C. Roberts and S. Rica, *Phys. Rev. Lett.* **102**, 025301 (2009).
- [29] W. Casteels, J. Tempere, and J. T. Devreese, *Phys. Rev. A* **86**, 043614 (2012).
- [30] F. Grusdt and M. Fleischhauer, *Phys. Rev. Lett.* **116**, 053602 (2016).
- [31] V. Shukla, M. Brachet, and R. Pandit, [arXiv:1412.0706](https://arxiv.org/abs/1412.0706).
- [32] C. Nore, M. Abid, and M. E. Brachet, *Phys. Fluids* **9**, 2644 (1997).